Combustion and Flame 192 (2018) 59–70

Contents lists available at ScienceDirect

Combustion and Flame

journal homepage: www.elsevier.com/locate/combustflame

Aluminized composite propellant combustion modeling with Heterogeneous Quasi-One dimensional (HeQu1-D) approach

S. Varunkumar[a,*], H.S. Mukunda[b]

[a] Department of Mechanical Engineering, Indian Institute of Technology Madras, Chennai 600036, India
[b] CGPL, Department of Aerospace Engineering, Indian Institute of Science, Bangalore 560012, India

ARTICLE INFO

Article history:
Received 17 September 2017
Revised 30 October 2017
Accepted 24 January 2018

Keywords:
Aluminum
Catalyst
Composite propellants
Radiation
Modeling

ABSTRACT

The Heterogeneous Quasi One-dimensional (*HeQu1-D*) model for AP/HTPB composite propellant combustion is extended to aluminized propellants. Following the serial burning approach of *HeQu1-D*, a statistical particle path through an aluminized propellant is taken to consist of aluminized binder-matrix coated AP particles of various sizes. Extending the idea of homogenization of fine-AP particles, aluminum particles are assumed to be homogenized with the binder-matrix. Large Al particles (nominal size $\geq$ 15 μm) in the binder-matrix are assumed to get ejected into the gas phase and hence do not contribute to heat feedback to the burning surface. With these modifications, the model is shown to accurately predict the burn rate variation with pressure and initial temperature of propellants using Al of nominal sizes in the range of 15–50 μm (termed conventional aluminum, CAl). The experimentally observed reduction in propellant burn rate with substitution of AP by CAl is shown to be due to the increase in fuel richness and energy sink effect of melting of Al. Catalytic effects due to addition of burn rate modifiers (Fe_2O_3 in space shuttle booster propellant, for instance) are also accounted for by modifications to gas phase rate parameters. Increase in burn rate up to 25% with Al particles of a few μm (3–6 μm) in comparison with non-aluminized propellant is explained by recognizing that there will be non-negligible fraction of sub-micron Al due to the associated particle size distribution. This leads to heat release by sub-micron Al combustion close to the surface and an enhancement in the heat feedback, by a combination of convective and radiative mechanisms. Dramatic increase in burn rate with sub-micron Al (a factor of 4–5 as compared to CAl) is captured by invoking radiation from fine-Al/Al_2O_3 particles to propellant surface. Agglomeration of sub-micron Al particles is invoked to explain the saturation of burn rate enhancement with reduction in Al particle size and the effectiveness of sub-micron Al substitution in smaller fractions (bi-modal Al). Predictions for over fifteen different propellants with varying fractions of fine and coarse aluminum from earlier literature have been presented. Comparisons of the predictions from the model with experimental results from different sources is shown to be excellent-to-good for most cases. The hitherto unknown radiation dominated ablation ($\dot{r} > 50$ mm/s) of coarse AP particles and the effect of Al particle size on propellant temperature sensitivity are brought out. The MATLAB® code based on the model offers opportunity for design of AP-HTPB composite propellants with combination of fine and coarse aluminum with confidence.

1. Introduction

Aluminum fraction in composite propellants varies between 18% (launch vehicle class) to a few % (smokeless tactical missile class). Nominal aluminum particle sizes used in typical application propellants vary from 15 to 50 μm, with 25 μm being the commonly used size, termed conventional aluminum (CAl). Smaller Al sizes are mostly used only in laboratory research - for instance, the 5.65, 5 and 3 μm used in [1–3] respectively. Insight into the effect of substitution of AP with conventional (15–25 μm) and smaller size (a few μm) Al can be obtained by comparing the burn rates of the following propellants - one non-aluminized with 86% AP (Mix-I from [4]), other two aluminized with 68% AP and 18% Al (C1 - 25 μm Al and C2 - 5.65 μm Al from [1]) (all three have same AP distribution). Burn rates of these three propellants taken from [1,4] are shown in Fig. 1.

Burn rate of propellant C1 with 25 μm Al is lower than Mix-I by 23% at 70 atm and has a pressure index of 0.33 compared to 0.44

* Corresponding author.
E-mail address: varuns@iitm.ac.in (S. Varunkumar).

https://doi.org/10.1016/j.combustflame.2018.01.042
0010-2180/

Nomenclature

$\dot{q}_R$	radiative flux (W/m^2)
$\dot{r}$	linear burn rate (mm/s)
σ_p	temperature sensitivity (%/K)
d_0	diffusion distance (μm)
d_{AP}	AP particle diamter (μm)
d_{pm}	premixed cut-off diamter (μm)
F_i	mass fraction of component *i* in aluminized binder-matrix
f_i	mass fraction of component i
g_f	geometric factor
H_s	surface enthalpy change (kJ/kg)
K_r	gas phase reaction rate (s/m^2-atm)
l_i	line average fraction
T_0	initial temperature (K)
T_f	flame temperature (K)
T_s	surface temperature (K)
t_{bm}	binder thickness (μm)
T_{eff}	effective gas phase temperature (K)
x^*	flame standoff distance (μm)
ABM	aluminized binder-matrix
BRM	burn rate modifiers
CAl	conventional aluminum
UFAL	ultra fine aluminum

of Mix-I. It is clear that the substitution of AP by CAl reduces the burn rate and index. It is important to note that the AP/HTPB ratio of Mix-I (86/14 = 6.1) is closer to stoichiometry (88/12 = 7.33) compared to that of C1 (68/14 = 4.9). This increase in fuel richness of C1 combined with the energy sink effect due to melting of Al particles at the surface of the propellant is later used to predict its burn rate behavior. On the other hand propellant C2 from [1] with 5.65 μm Al in place of CAl burns at a rate comparable to Mix-I (non-aluminized) at all pressures, in spite of the fuel richness and Al energy sink effect brought out earlier. This is argued to be due to heat release from the sub-micron fraction in 5.65 μm Al used in C2. Ishihara et al. [2] obtained experimental results by systematically substituting 5 μm Al in bi-modal AP/HTPB propellant with 82% total solids (A-0, 5, 10, 20 in Fig. 1). The burn rate data, though limited, is consistent with that from [1] - substitution of 5 μm Al for AP has marginal effect on burn rate. Therefore the effects of fuel richness due to decrease in AP fraction and the Al melting related surface energy sink effects seem to be counteracted by Al particle related processes in the gas phase. Ishihara et al. [2] have shown that the radiation received by propellant A-20 (with 20% 5 μm Al) is about 20% of the gas phase flux at 35 atm - this is consistent with the observation about sub-micron fraction oxidation close to the surface for 5 μm Al. For Al nominal sizes of 15 μm and above since the sub-micron fraction is negligible the compensating mechanisms are absent leading to decrease in burn rate compared to the non-aluminized counterpart. Thus Al particles of nominal size about 5 μm and less cannot be classified as CAl. Results from extensive experimental studies by Price and group (see for instance [5,6]) are also consistent with these observations - with use of 3 μm aluminum leading to burn rate increase by 35% at 69 atm compared to propellants with 15 and 30 μm aluminum. The corresponding non-aluminized compositions (89% AP) were not considered in [6]. But predictions for the non-aluminized compositions were obtained using the HeQu1-D model and the results show that the burn rates of compositions with CAl (15 and 30 μm Al) are 20% lower and that of the compositions with 3 μm Al is 15% higher than the non-aluminized cases, consistent with the observations made so far. Pressure index also increases with

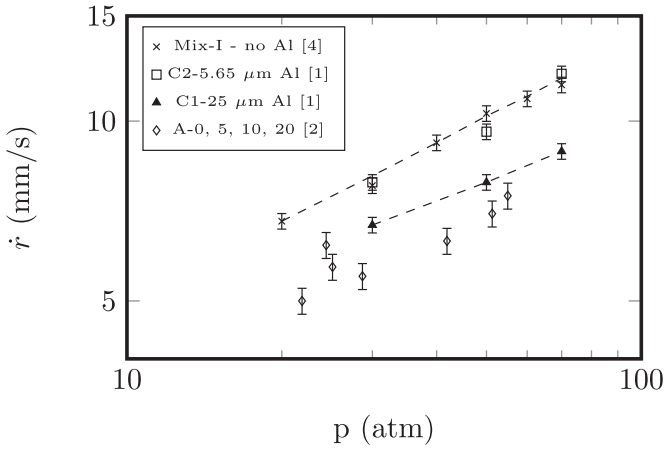

Fig. 1. Effect of substitution and particle size of Al for AP refs [1,2,4]; error bar is 3% for data from [1,4] and 5% for [2].

replacement of 30 μm Al with 3 μm Al from about 0.3 to 0.48 consistent with earlier observation related to propellants from [1,4]. Note that differences in burn rate index in general are difficult to quantify compared to burn rate itself.

Recent interest in high burn rate propellants ($\sim$ 40 mm/s) has led to the use of ultra-fine aluminum (UFAl) which belongs to sub-micron sizes. Studies due to Dokhan et al. [6] on propellants of 89% total solids with 18% aluminum indicate that use of UFAl can increase the burn rate of propellant dramatically - a factor of 5 compared to propellants with CAl. Even 20% substitution of CAl with UFAl is shown to lead to three times increase in the burn rate as compared to CAl propellants indicating a shift in the combustion mechanism as compared to propellants with CAl.

These observations on the effect of aluminum particle size can be rationalized and predicted using a modeling framework by incorporating the following two points - (1) ignition of Al is a strong function of particle size and oxide coating (purity) and (2) Al added to any propellant has an associated size distribution (usually log-normal as found for space shuttle Al [7]). Arguments are presented later to show that, almost all of conventional Al particles (nominal 15 μm and above) ignite sufficiently far away from the propellant surface to have any significant influence on the convective and radiative fluxes to the propellant surface leading to a burn rate decrease compared to the non-aluminized propellant. As the nominal size is decreased, the fraction of sub-micron Al oxidizing sufficiently close to the surface increases (due to the associated particle size distribution) and contribution to the heat flux to the surface increases leading burn rate increase compared to CAl propellants - propellants with 3, 5 and 5.65 μm Al from [1,2,6] are cases in point. At sub-micron nominal sizes all of the aluminum will oxidize very close to the surface causing dramatic increase in burn rate - as shown later, almost all the heat flux with UFAl comes from radiation due to the inverse dependence of radiative flux on Al particle size. Rupture of oxide coating due to volume expansion caused by melting of aluminum core in sub-micron sized particles is a possible ignition mechanism of UFAl particles (see [8,9]). This mechanism is clearly dependent on the surface-to-volume ratio and hence can become dominant at sub-micron scales. Similar considerations are applicable to high surface area flaky aluminum with thickness of few tens of nanometers which are shown to enhance burn rates compared to CAl by a factor of about 2.5 in [1]. By incorporating these additional features, the recently developed '*Heterogeneous Quasi One-dimensional (HeQu1-D) model*' [10] for non-aluminized propellants is extended to account for aluminum effects. Catalytic effects due to addition of burn rate modifiers (Fe_2O_3, for instance) are also accounted for by

modifications to gas phase rate parameters (a detailed discussion is presented later). Burn rate predictions as a function of pressure and initial temperature are presented.

1.1. Earlier models

Apart from burn rate measurements, many studies on aluminized propellants have focused on understanding and controlling agglomeration (see for instance [5,11–14]) and combustion of single aluminum particles [15,16]. The combustion studies however, are under conditions far from those being experienced near a burning surface (see [15,17,18]). To the best of our knowledge, a model for predicting the steady combustion behavior of composite solid propellants including aluminum is not available; we recognize that Lengelle et al. [19] have carried forward the serial burning approach of Beckstead [20], but the methodology was not carried forward to include physics needed for converting the idea into a predictive tool. While results of the single particle Al combustion studies, both experimental and modeling, provide insights to develop burn rate models for aluminized propellants, the current approach utilizes the *HeQu1-D* framework, extended to account for changes in thermo-chemistry and heat transfer mechanism with associated Al particle size effects like agglomeration incorporated using a simple analytical approach.

The *HeQu1-D* model combines the serial burning approach with a quasi-1D burn rate model for binder-matrix coated AP particles to calculate the propellant burn rate ($\dot{r}$) as the reciprocal of the burn time of a statistical particle path of unit length. The burn time is calculated as sum of contributions from each binder-matrix coated AP particle constituting the statistical particle path, which is the ratio of the line average fraction of each particle to the corresponding burn rate. Premixed-limit and extinction-cut-off are the two ideas incorporated in the *HeQu1-D* model and shown to be critical to its predictive capability (see [10] for more details). The homogenized binder composed of HTPB and AP particles smaller than the premixed- and extinction-cut-off limits is assumed to be apportioned in such a way that the AP particles are coated with uniform thickness; this approach of binder-matrix distribution being a strategy for arriving at the representative O/F distribution and line average fractions in a propellant. Ignoring the actual thickness in diffusion distance estimate (eq. 16 in [10]) has insignificant effect on the final results. In this paper this framework is extended to account for the effects of aluminum.

Predicted burn rate variation with pressure from the extended model is shown to compare well with experimental results for a number of aluminized propellants chosen from literature. It is pertinent to point out that the predictions correspond to propellants burning as individual strands (note, for TPH1148 the information on the measurement method is not available) and not in rocket motor conditions (additional burn rate augmentation effects due to far field radiation etc., are not dealt with here). As far as effect of initial temperature (T_0) is concerned, the important conclusion drawn from the closed form expression in [10] (eq. 18) is that the temperature sensitivity (σ_p) of a composite propellant containing only AP and HTPB will be lower than that of the AP used. It is important to note that earlier theoretical results of Cohen-Nir [21], Cohen and Flanigan [22] lead to the same conclusion. Even so, the generally reported σ_p values for AP/HTPB composite propellants vary widely - for instance the values for 87.4% AP/HTPB propellants studied by Blomshield and Osborn [23] is seen to vary between 0.17 and 0.32 %/K at 68.9 atm, while that of pure AP reported in [24] is 0.16 %/K at 68.9 atm. As brought out earlier in [10] it is inferred that this is due to the trace impurities invariably present in AP - usually potassium ions (K^+) which is known to significantly increase the temperature sensitivity (up to 1 %/K as shown in [24]). That this is the reason for the apparent conflict between theory and data has been left unattended in all of the earlier works. Therefore, unless AP temperature sensitivity is reported along with that of the propellant, something that has not been done, quantitative comparison with theoretical predictions will be of limited value and this applies equally for aluminized propellants as well. Yet, σ_p results are presented and discussed here along with limited experimental comparison. The role of Al in modifying the temperature sensitivity of propellants is brought out using the crucial Al particle size effect and the interplay between surface temperature and radiative flux on burn rate variation with initial temperature. From the practical point of view, these considerations point to the possibility of using ultra-pure AP as a simple solution for obtaining low σ_p, a desirable quality for practical propellants.

The rest of the paper is organized as follows - 1) effect of conventional Al, 2) effect of sub-micron Al (UFAl), 3) temperature sensitivity of aluminized propellants, 4) free parameter determination via calibration and 5) conclusions.

Table 1
Composition and burn rate of propellant TP-H1148 (Space shuttle booster propellant).

Composition	
AP	69.72% (nominal 200 μm from Kerr-McGee)
Al	16% (nominal 50 μm from Alcoa)
Fe_2O_3	0.28%
Ballistic properties	
$\dot{r}$ at 68.9 atm	10.7–11.9 mm/s*
Index, n	0.35*
Temperature sensitivity, σ_p	0.11 %/K*

* - from [32].

2. Effect of conventional aluminum

The modifications required to account for the effect of CAl are explained in this section using the example of space shuttle booster propellant (TP-H1148). The composition and ballistic data for this propellant is given in Table 1.

The particle size distribution for AP is available from [25] and is found to be very close to that of the 200 μm AP reported in [26] (also from Kerr-Mcgee). The particle size distribution for Al from Alcoa is available from [7] - the distribution is log-normal (like AP) with a mean size of 50 μm and a SD of 45 μm - a very wide distribution.

Application of HeQu1-D model to predict the burn rate of a propellant involves the following steps - (1) construction of the statistical particle path and calculating the associated thermo-chemistry and (2) particle burn rate calculation using quasi 1-D equations.

2.1. Statistical particle path

1. The first step in HeQu1-D is the construction of the *statistical particle path* using the serial burning approach. This begins with the calculation of fraction of AP particles smaller than the premixed-cut off (given by $d_{pm} = 16e^{-0.02p}$, where d_{pm} is the premixed cut-off size in μm and p is pressure in *atm* ([10]). The smallest AP particle in TPH1148 is about 20 μm and since d_{pm} is 11 μm at 20 atm and 4 μm at 70 atm, the fraction smaller than the premixed cut-off size (d_{pm}) is zero. Therefore the initial fraction of fine-AP is zero. Aluminum and catalyst are added to the binder (PBAN for TPH1148) and following the HeQu1-D model, the apportioning of this *aluminized binder-matrix (ABM)* amongst AP particles of different sizes is calculated by assuming that the volume of aluminum-binder mixture is coated with uniform thickness on AP particles. The fraction of AP, HTPB, Al and burn rate modifiers (*BRM*) in the aluminized binder-matrix

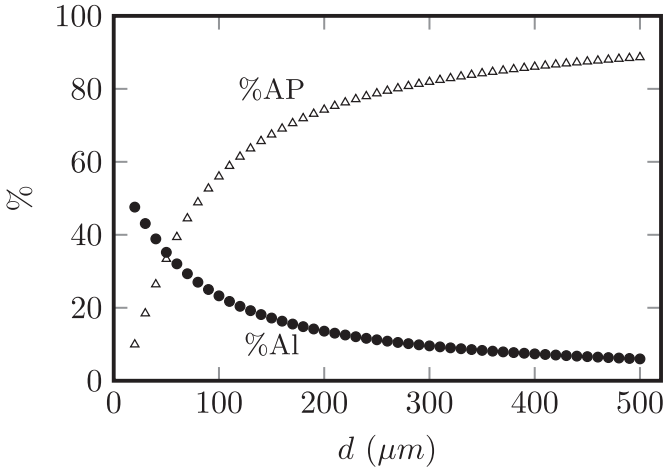

Fig. 2. AP and Al fraction as a function of particle diameter for TPH1148 propellant.

is denoted as F_{AP}, F_{HTPB}, F_{Al} and F_{BRM} respectively. With a binder fraction of 14% and CAl fraction of 16%, the density of the aluminum-binder mixture is 1440 kg/m^3 and when coated uniformly over AP particles, the resulting thickness (t_{bm}) is 14 μm (using Eq. 1).

$$\frac{f_{HTPB}}{\rho_{HTPB}} + \frac{f_{pm}+f_{ex}}{\rho_{AP}} + \frac{f_{Al}}{\rho_{Al}} + \frac{f_{BRM}}{\rho_{BRM}} = \sum_{i=1}^{n} \frac{f_i[(1+2t_{bm}/d_i)^3 - 1]}{\rho_{AP}} \tag{1}$$

where, f and ρ denote mass fraction and density of different components (pm - premixed cut off AP, ex - extinct AP - more details later, BRM - burn rate modifiers), d_i is the diameter of different AP particles from the input distribution and t_{bm} is the thickness. The statistical particle path is taken to consist of AP particles of various sizes, each coated with a thickness of t_{bm}. The fraction of the line composed of particles of various sizes (l_i) is proportional to the volume fraction of corresponding size and calculated using Eq. 5 from [10]. With this the propellant burn rate can be calculated as the ratio of the length of the statistical particle path to the corresponding burning times - $\dot{r} = [\sum l_i/\dot{r}_i]^{-1}$, where $\dot{r}_i$ is the burn rate of binder-matrix coated AP particles constituting the statistical particle path (see Eq. 6 in [10]).

2. With t_{bm}, the mass fraction of AP, Al, BRM and HTPB for each particle can be calculated using (Eqs. 2,3)

$$f_{AP,d_i} = \frac{\rho_{AP} + \rho_{bm}\left[(1+2t_{bm}/d_i)^3 - 1\right]F_{AP}}{\rho_{AP} + \rho_{bm}\left[(1+2t_{bm}/d_j)^3 - 1\right]} \tag{2}$$

$$f_{j,d_i} = \frac{\rho_{bm}\left[(1+2t_{bm}/d_i)^3 - 1\right]F_j}{\rho_{AP} + \rho_{bm}\left[(1+2t_{bm}/d_j)^3 - 1\right]} \tag{3}$$

where, ρ_{bm} is the density of the *aluminized binder-matrix* (ABM) given by Eq. (4), F_j is the mass fraction of component j (j = Al, HTPB or BRM) in ABM.

$$\rho_{bm} = \frac{f_{HTPB} + f_{pm} + f_{ex} + f_{Al} + f_{BRM}}{f_{HTPB}/\rho_{HTPB} + (f_{pm}+f_{ex})/\rho_{AP} + f_{Al}/\rho_{Al} + f_{BRM}/\rho_{BRM}} \tag{4}$$

In Fig. 2 the %AP and %Al are shown for the propellant TPH1148 at 20 atm.

In calculating the flame temperature using NASA-CEA, the CAl particles are assumed to be inert and the energy absorbed by the Al particles due to heating in the flame zone close to the propellant surface is also neglected. Justification for these two assumptions is as follows - the typical conduction time (r^2/α) for an Al particle of 50 μm diameter with a thermal diffusivity (α) of 100 mm^2/s will be 6.2 μs. This is larger than the time of flight of particles through the flame zone - which, as shown in Table 2 is less than 4 μs at 20 atm and less than 2.5 μs at 70 atm for TPH1148 (details of calculation of time of flight are discussed later). The maximum flame thickness corresponding to the time of flight (shown in Table 2) is 8.3 μm and 2.5 μm for 500 μm AP particle at 20 and 70 atm in TPH1148 propellant. Therefore the state of a typical Al particle as it leaves the flame zone is perhaps just melted. Even for the smallest CAl nominal size of 15 μm, though the conduction time is only about 0.6 μs, for it to ignite the outer Al_2O_3 coating must melt requiring a temperature of more than 2300 K. Given that a 15 μm Al droplet takes about 1 ms to burn (assuming d^2 to be approximately valid with a burning constant of 0.3 mm^2/s from [15]), the fraction of Al burning close to the surface is negligibly small. These considerations allow for CAl particles to be treated as inert with negligible heat up in the equilibrium flame temperature calculations.

Table 2
Calculated flame thickness (x^*) and time of flight of Al particles (t_f) for propellant TPH1148.

d_i (μm)	20 atm		70 atm	
	x^* (μm)	t_f (μs)	x^* (μm)	t_f (μs)
500	8.3	3.8	2.5	2.3
250	5.2	1.5	1.8	1.4
100	5	3.2	1.2	0.86
50	ext*	ext	1.0	1.8

* - extinguished AP particles, $T_s < 870$ K.

2.2. Burn rate of binder-matrix coated AP particles

To calculate the propellant burn rate, the burn rate of individual aluminized binder-matrix coated AP particles constituting the statistical particle path is required. The *quasi 1-D* approach for non-aluminized propellants developed in [10] is extended to aluminized propellants here. The derivation of the burn rate equation begins with the heat flux balance at the surface given in

$$k\left[\frac{dT}{dx}\right]_{0^-} = \rho_p \dot{r} H_s + k\left[\frac{dT}{dx}\right]_{0^+} \tag{5}$$

where, the LHS is the condensed phase flux and the second term on the RHS is the heat flux to the surface from the gas phase flame. The surface enthalpy change (H_s) accounts for the decomposition/melting of the ingredients (AP, HTPB, Al etc.) and is calculated using the following expression

$$H_{s,i} = f_{AP,i}H_{AP} + f_{HTPB,i}H_{HTPB} + f_{Al,i}H_{Al}$$

where, $H_{AP} = 0.6p\ \ (atm) + 500$ kJ/kg and $H_{HTPB} = -600$ kJ/kg (taken from [10]) and H_{Al} is the enthalpy of melting of Al (−346 kJ/kg). From Eq. (5), the burn rate equation (Eq. 6 shown below) is obtained from the solution of the condensed and gas phase temperature profiles (details available in [10]).

$$\rho_p \dot{r}_i = \sqrt{\frac{k_g}{c_p}\, K_{r,eff,i}\, p^2\, ln\left(\frac{T_{eff,i} - T_{s,i}}{T_{s,i} - T_0 - H_{s,i}/c_p} g_{f,i}\right)} \tag{6}$$

where, $\dot{r}_i$ is the particle burn rate, c_p is the specific heat (assumed constant and equal for condensed and gas phase, 1150 J/kg-K), k_g is the thermal conductivity of gas phase (assumed constant at 0.08 W/m-K), $K_{r,\,eff,\,i}$ is the effective gas phase reaction rate, $T_{eff,\,i}$,

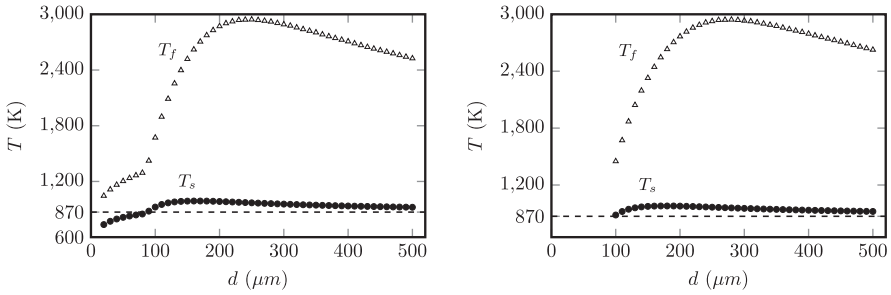

Fig. 3. Flame and surface temperature of binder-matrix coated AP particles in propellant TPH1148 at 20 atm without and with extinction.

$T_{s,\,i}$ and T_0 are the effective gas phase, surface and initial temperature of particle of size d_i and $g_{f,i} = d_i^2/(d_i + 2t_{bm})^2$ is the geometric factor. The reaction time limited diffusion distance (d_0) based methodology developed in [10] for calculating $T_{eff,\,i}$ and $K_{r,\,eff,\,i}$ is used here as well. The non-dimensional variable $Z = d_{AP}/d_0$ with $d_0 = \sqrt{D\ t_r}$ (D - mass diffusion coefficient and t_r - characteristic reaction time) used to calculate the extent of lateral diffusion is related to the second Damkohler number, $Z = \sqrt{Da_{II}}$. Procedure for estimating d_0 and Z are same as in [10].

The calculated flame and surface temperature for TPH1148 at 20 atm is shown in Fig. 3(a). Surface temperature of particles up to about 100 μm is less than 870 K - the melting temperature of AP and the minimum temperature required for self-deflagration. This intrinsic limitation for AP self-deflagration was used in [10] as the criteria for '*local extinction*'. Such extinct particles are homogenized with the binder-matrix and an iterative procedure is used till all particles have surface temperature $\geq$ 870 K. The final result for TPH1148 at 20 atm is shown in Fig. 3(b). It is possible that for certain compositions under some range of pressures, all particles might have surface temperature lower than 870 K and this is taken to imply global extinction. The flame thickness (x^*) and corresponding time of flight (t_f) for AP particles of various sizes in TPH1148 are calculated using Eq. (7) and shown in Table 2.

$$x^* = \frac{\rho_p \dot{r}}{K_{r,eff} p^2}; \quad t_f = \frac{x^*}{v_g} = \frac{1}{RT_{eff} K_{r,eff} p}; \tag{7}$$

where, v_g is the characteristic gas phase velocity.

The surface temperature predictions and other results presented so far for TPH1148 propellant include the effect of catalyst (Fe_2O_3) as well. The details of the modifications incorporated to account for catalytic effects are presented in the following section.

2.3. Effect of catalyst

The way burn rate modifiers work differs between those that reduce the burn rate and those that enhance it. That the burn rate inhibitors not only depress burn rate but also significantly reduce burn rate index (beyond that can be explained by diffusion effects) indicate significant changes in the near surface behavior [10]. Catalysts, like IO and CC show significant enhancement at just 0.5%, while inhibitors show perceptible effect at only a few % substitution. Also inhibitors are compounds which either melt or decompose at temperatures comparable to that of the propellant surface. On the other hand, melting temperature of IO is above 1800 K and the catalytic activity of CC is likely to be due to the oxides of copper formed at temperatures above 1300 K - characteristic of gas phase conditions. This is clearly indicative of largely gas phase action in the case of catalysts. The gas phase pathways are altered to effectively reduce the activation energy of gas phase reactions (E_g) and enhance the reaction rate (K_r) and the gas phase flux. The magnitude by which K_r must be increased, as described in [10], can be obtained from the enhancement in burn rate of a fine-AP/binder with addition of catalyst. Critical concentration at which the catalytic effect saturates can also be obtained using this technique. The burn rate enhancement is a function of the catalyst particle size - nano sized particles are known to enhance burn rate more significantly than micron size particles, as the number of active reaction sites are much higher in high surface area nano particles compared to micron sized particles. There is also a critical catalyst fraction beyond which the catalytic effect saturates - data from [27] shows that for an aluminized propellant with 86% total solids, the catalytic effect saturates at 1% with micron sized Fe_2O_3 (5–20 μm); beyond 1% the burn rate starts to decrease. This observed saturation of the catalytic effect could be due to a combination of two factors - 1) largely kinetic limitations associated with dynamics of active sites for reactions (and hence the dramatic difference between micro and nano-size particles at same concentration) and 2) to a lesser extent, the reduction in total energy and hence effective flame temperatures as the fraction of inert catalyst particles is increased.

Fine-AP/binder propellant with 86% AP burns at 18 mm/s at 20 atm [10,28]. This was used to deduce the gas phase reaction rate ($K_{r,\,86\%} = 30{,}000$ s/m^2-atm) by using the 1-D burn rate equation (see Table 1 in [10]). Substitution of 1% Fe_2O_3 used in TP-H1148 is assumed to lead to enhancement in burn rate to 24 mm/s. Using this the gas phase reaction rate is deduced using the same procedure to be 57,551 s/m^2-atm. Addition of 1% Fe_2O_3 is assumed to cause only a negligible change in the flame temperature. If a certain quantity of catalyst is mixed with the binder, appropriation of binder-matrix amongst AP particles imply that the mass fraction of catalyst varies as a function of AP particle size - concentration of catalyst will be higher in fuel rich smaller particles compared to AP rich larger particles. To account for this, the gas phase reaction rate (K_r) is assumed to be a linear function of the catalyst concentration - this is found to be reasonable as the catalyst fraction usually is in a narrow range of 0 – a few %, beyond which the effect saturates. Beyond the saturation point, the reaction rate is assumed to remain constant (at corresponding flame temperatures). The *HeQu1-D* model implemented in MATLAB® is extended to incorporate these additional features and burn rate results are obtained. Figure 4(a) shows a plot of the predicted burn rates for the space shuttle booster propellant (TP-H1148) and can be seen to match closely with experimental results (within $\pm 5\%$). Further experiments with fine-AP/HTPB propellants are required to validate the assumed enhancement in burn rate (18–24 mm/s with 1% Fe_2O_3). Results for the effect of micron and nano sized Fe_2O_3 on aluminized propellants from [27] along with predictions are shown in Fig. 4(b). A burn rate enhancement to 30 and 45 mm/s from the base value of 18 mm/s with substitution of 1% micron (5–20 μm) and nano (30 nm) sized Fe_2O_3 particles for 1% AP in fine-AP/HTPB propellant respectively is seen to capture the catalytic effect accurately. While several hypothesis for site of action of catalyst have

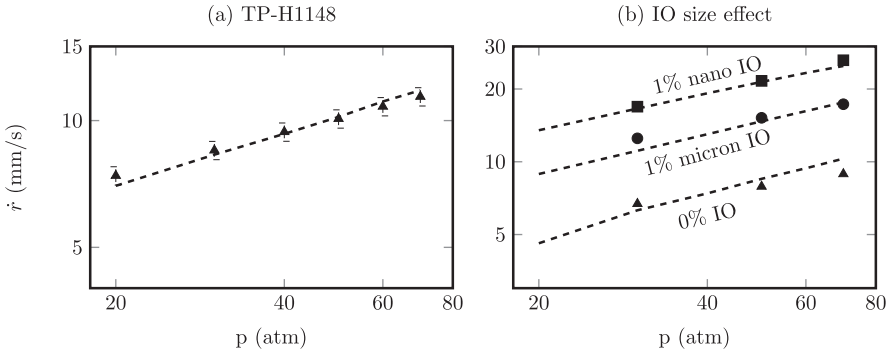

Fig. 4. Predicted vs experimental burn rate for space shuttle booster propellant, TP-H1148 (error bars correspond to ±5%) and propellants from [27].

been proposed in the past (a summary can be found in [4]), to the best of our knowledge, this is the first time the effect has been captured using a modeling framework. That the catalysis of the gas phase reaction between decomposition products of AP and binder is the predominant route for burn rate enhancement is satisfactorily demonstrated.

Dokhan et al. [6] has reported experimental burn rate measurements for a number of compositions by systematically varying the AP coarse to fine ratio and with Al sizes 0.1, 3, 15 and 30 μm. Predicted vs experimental burn rate for 8 bi-modal AP (400 μm and 82.5/10 μm) are shown in Figs. 5 and 6. These results were obtained by assuming that 60% of 3 μm Al and none (0%) of 15 and 30 μm fall in the fine-Al category. Since the actual particle size distribution for 3 μm Al is not available, the active fraction numbers are arrived at to get a good fit of the data. A robust methodology for estimating this fraction should be based on the fine-AP/HTPB/Al propellant burn rate data and the particle size distribution of Al. This would also enable the conductive and radiative fluxes to be independently estimated. It is interesting to note that the assumption of 60% active component in 3 μm Al is qualitatively consistent with the visual observations of the aluminum-burning region (ABR) reported by Dokhan et al. [6] - a distinct increase in the luminosity of the ABR was observed with 3 μm Al compared to 15 and 30 μm Al indicative of ignition of a fraction of Al particles close to the propellant surface. Also the ABR with 3 μm Al is reported to be similar to that with UFAl (0.1 μm). As shown later, with significant amount of sub-micron Al the radiation becomes a dominant factor - indicating that the increase in particle number density for sub-micron Al (a factor proportional to the cube of the particle size ratio) is responsible for this shift in combustion mechanism. The predictions for propellants in Fig. 5 containing bi-modal 400 and 82.5 μm are excellent to good. Out of the four propellants with 400 and 10 μm AP, predictions for which are shown in Fig. 6, two show good comparison while the other two are not unreasonable. Given that the 400 and 82.5 μm AP used were as received from WECCO (earlier Kerr-McGee) for which detailed particle size distribution is available from [26] and 10 μm AP used in [6] was obtained from elsewhere (US Naval Warfare Center, China Lake as indicated in [3]) the overall performance of the model is good. The reported results were obtained by assuming a log-normal distribution with a mean size of 10 μm and a SD of 1 μm. In Fig. 7 predictions vs experiments are shown for propellants reported in [1,29].

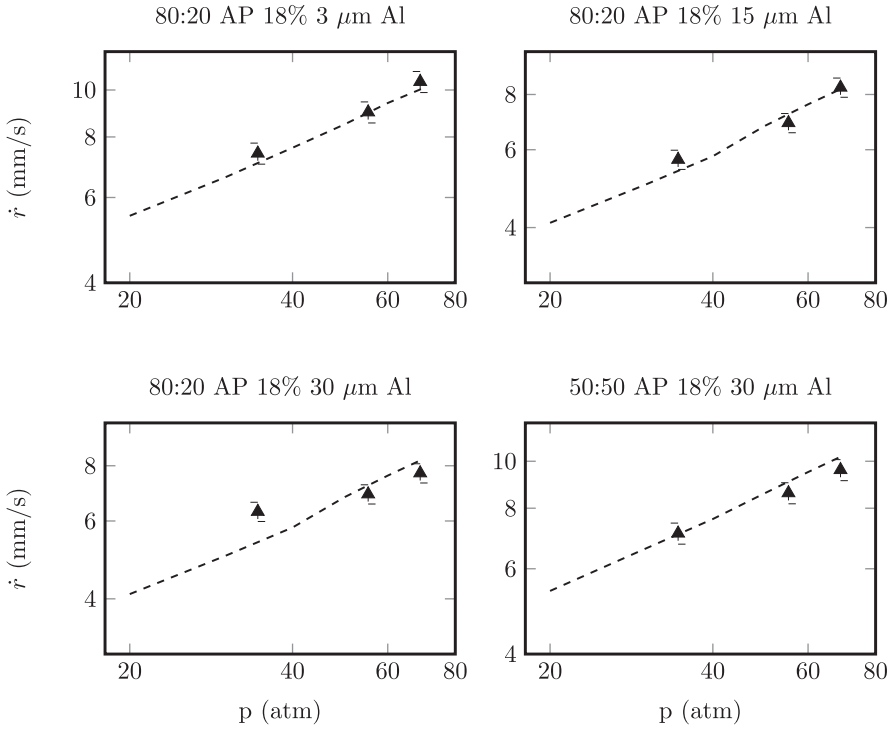

Fig. 5. Predicted vs experimental burn rate for propellants from Dokhan et al. [6] - bi-modal AP (400/82.5 μm) with different Al sizes as indicated above the plots.

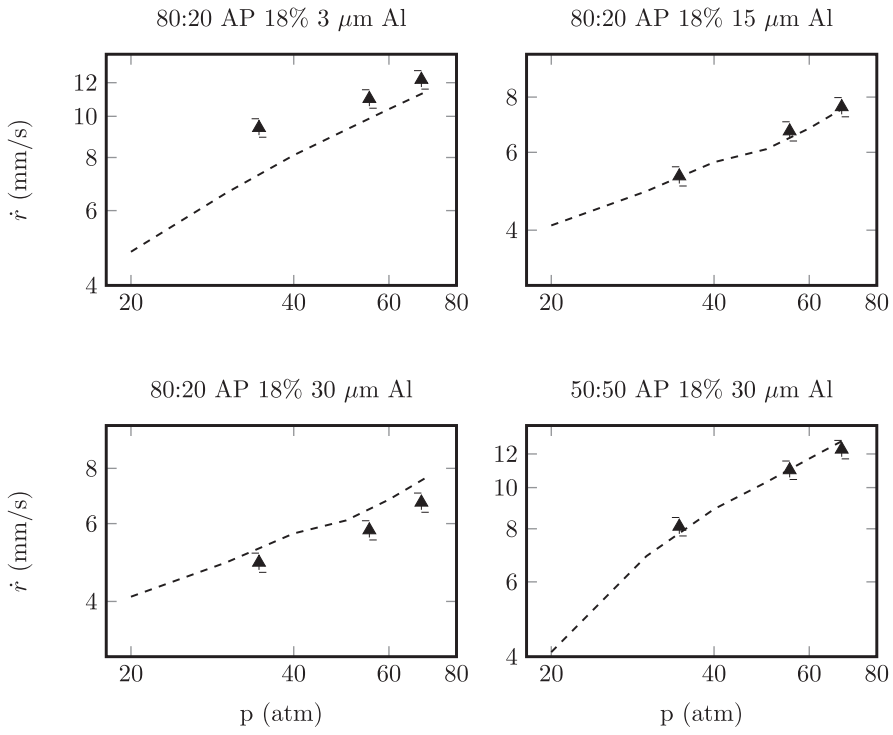

Fig. 6. Predicted vs experimental burn rate for propellants from Dokhan et al. [6] - bi-modal AP (400/10 μm) with different Al sizes as indicated above the plots.

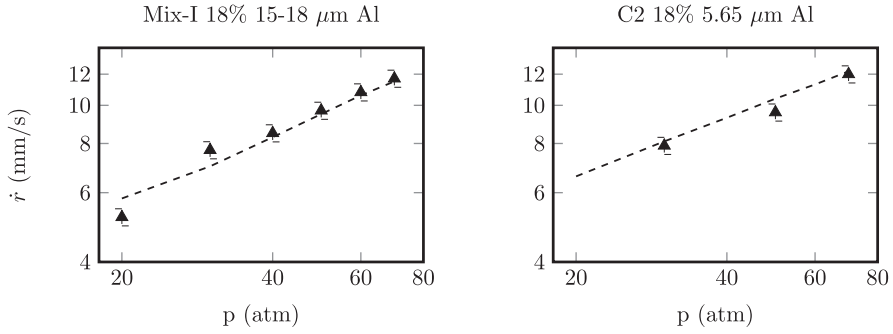

Fig. 7. Predicted for experimental burn rate for propellant from Verma and Ramakrishna [29] (Mix-I - SHAR AP) and Verma and Ramakrishna [1] (C1 and C2 - sieved TCL AP). All three propellants have 68% AP (1:1 coarse to fine) and 18% Al.

For 15–18 μm Al used in Mix-I, 10% is assumed to be active. None of 25 μm Al (in C1) and 20% of 5.65 μm Al (in C2) were assumed to be active. The comparison is excellent for Mix-I and C2 and can be considered good for C1 (0% IO case shown in Fig. 4(b)).

2.4. Neglect of radiation for CAl

In the context of the current work comparison of model predictions are sought with experimental results for aluminized propellant strands. The data shown in Fig. 1 indicates that substitution of AP with CAl ($\geq$ 15 μm) particles reduces the propellant burn rate by 20%. The model predictions presented so far clearly show that this reduction is due to the increase in fuel richness due to substitution of AP by Al and the energy sink effect due to Al melting. This observation based on the theory and model predictions is consistent with the earlier observation that the fraction of CAl consumed in the flame zone is negligible. Also for a typical aluminized propellant (68% AP and 18% Al of 15 μm size), about 70 million particles are ejected per cm^2/s corresponding to a burn rate of 10 mm/s, making the surface opaque. Moreover under strand-burning conditions the fraction of radiation intercepted by the propellant surface, even in the absence of an intervening medium will decrease with distance from the surface. Essentially radiation from CAl particles reaching the surface cannot play any role in determining the burn rate of the propellant strand. On the other hand non-negligible sub-micron fraction of nominal 3, 5 and 5.65 μm Al particles used in [1,2,6] burn close enough to the surface and depending on the associated distribution, use of these sizes can compensate for fuel richness and energy sink effects due to Al addition (like for propellants C2 from [1] and A-5, 10, 20 from [2]) or even enhance the burn rate (like for propellants from [6]). The contribution from these fractions burning close to the surface will be a combination of convective and radiative fluxes - the precise split up can be estimated only with the detailed particle size distribution of Al. Hence particles with nominal sizes in the range of a few μm are not classified as CAl - perhaps these can be termed *intermediate sizes* to differentiate from conventional and sub-micron sizes.

3. Effect of sub-micron Al

As stated earlier, larger Al particles (CAl) do not play an active role in the processes close to the propellant surface and hence treated as inert in the gas phase from the thermo-chemistry

Table 3
UFAl particle size effects.

Source	d_{UFAl} (μm)	d_{CAl} (μm)	$\dot{r}/\dot{r}_0$ (%UFAl/%CAl) (at 70 atm)	n
De Luca et al. [30]	0.15 (S*)	30	1.9 (100/0)	0.42[b]
			1.8 (50/50)	0.46
			1.6 (20/80)	0.35[c]
			1.0 (0/100)	0.43
Dokhan et al. [6]	0.1 (S)	30	5.9 (100/0)	0.41
			4.5 (50/50)	0.52
			3.3 (20/80)	0.69
			1.0 (0/100)	0.27
Verma and Ramakrishna [1]	0.018 (S)	25	4.5 (100/0)	0.53
	0.025 (F*)		2.6 (100/0)	0.61
	0.032 (F)		2.3 (100/0)	0.58
	0.032 (F)		2.0 (100/0)	0.55
	-		1.0 (0/100)	0.33

* - S - spherical; F - Flaky; [b/c] - average of two/three trials taken from [30].

and heat transfer point of view. But sub-micron particles significantly increase the propellant burn rate and from the experimental results reported in literature ([1,6,30]) it is clear that the increase in burn rate is a strong function of Al particle size as well as purity. Burn rate enhancement due to replacement of conventional Al with sub-micron Al from various experimental studies is summarized in Table 3. Results reported in [30] show that replacing CAl by 0.15 μm Al particles doubles the burn rate of the propellant, while 0.1 μm Al particles used in [6] increase the burn rate by a factor of 4–5 compared to propellants with CAl. The conflicting features, namely that replacing 30 μm Al with 2.5 μm Al in [30] leading to negligible change in burn rate and results reported in [6] indicating a 20% increase in burn rate with 3 μm Al compared to 30 μm are suggestive of lower purity of Al used in [30] (< 90%). The observed changes in burn rate index with substitution of CAl with UFAl is also to be taken note of. Results from [30] show only marginal changes in n, perhaps due to relatively less Al activity indicative of lower purity as observed earlier. On the other hand, results from [1] show a clear increase in n with replacement of CAl with nano/flaky Al. Dramatic changes in burn rate index are seen in data from [3] - for propellants with 80/20 400/82.5 μm AP, 20% UFAl substitution increases the index to 0.69 from 0.27 (for 100% CAl). With further increase in UFAl the index decreases to 0.52 (for 50% UFAl) and 0.41 (for 100% UFAl). Propellants with 60/40 and 50/50 AP show marginal change in n with 20% UFAl substitution and then a sharp increase to about 0.7 with 50% substitution is observed in the data reported in [3] (experiments with 100% UFAl were not done, perhaps due to propellant processing issues). Given that there are processing issues with aluminized propellants made in lab scale batches, especially so with UFAl particles, and that the principal aim of experimental studies was to demonstrate the effectiveness of UFAl in enhancing burn rates, it is likely that only relative changes in $\dot{r}$ were taken to be of importance. This is perhaps why attention was not given to the changes in n in [6]. Therefore the comparisons presented later are to taken as moderately quantitative.

In the following section, the modifications to the propellant geometry and thermo-chemistry due to addition of fine-Al is presented. Later the burn rate equation accounting for radiation is derived and the predictions are presented.

3.1. Propellant geometry and thermo-chemistry

Like CAl, sub-micron Al is also homogenized with binder and fine-AP. The statistical particle path and associated quantities like fractions of various components are calculated using the same procedure used earlier. The crucial difference is in calculating the flame temperature with NASA-CEA. With sub-micron particles completely oxidizing close to the surface, these are treated as active components in calculating the flame temperature. Starting with the propellant 80:20 AP (400/82.5 μm) with 18% 30 μm Al (from Fig. 5), Dokhan et al. [3] replaced increasing fractions of 30 μm Al with 0.1 μm UFAl, 20%, 50% and 100% respectively. The calculated binder thickness for these three propellants are 11.4, 12.9 and 15.2 μm respectively and the flame temperature for 400 and 82.5 μm particle is shown in Fig. 8. As CAl is substituted with UFAl, the flame temperature of 400 μm AP particle increases from 2585 K (0% UFAl) through 2746 K (3.6% UFAl), 2940 K (9% UFAl) to 3169 K (18% UFAl). Similarly for 82.5 μm AP particle the temperature increases from 1672 K (0%) UFAl to 2513 K (18% UFAl). This increase in flame temperature with replacement of CAl with UFAl leading to significant radiation contribution to heat flux is the primary factor responsible for the observed burn rate enhancement. Burn rate equation accounting for this effect is derived in the following section.

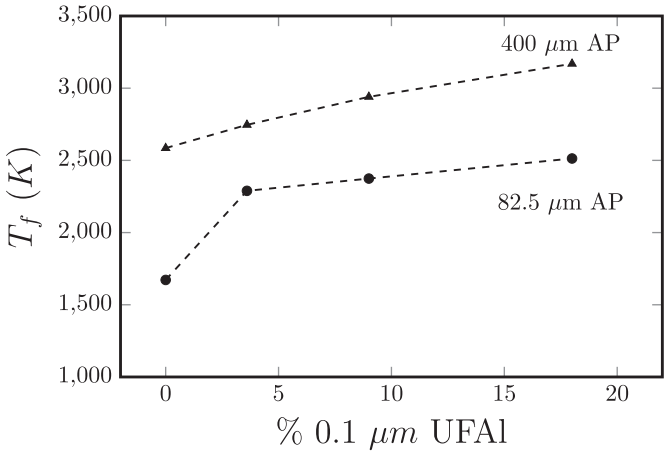

Fig. 8. Flame temperature increase with replacement of CAl with UFAl for representative particles in propellants from [6].

3.2. Burn rate equation for aluminized binder-matrix coated AP

The burn rate equation for aluminized binder-matrix coated AP particles is derived by starting with the surface heat balance as shown in

$$\rho_p \dot{r} c_p (T_s - T_0) = \rho_p \dot{r} H_s + \frac{\rho_p \dot{r} c_p (T_{eff} - T_s) g_f}{\exp[\rho_p \dot{r} c_p x^*/k_g] - 1} + \dot{q}_R \tag{8}$$

The notation used is same as earlier and in [10]. The third term on the RHS, $\dot{q}_R$, denotes the additive radiative flux to the propellant surface due to Al/Al_2O_3 particles in the gases. Simplification of Eq. (8) leads to Eq. (9), which has a form similar to that of Eq. (12) in [10] with an additional radiation term.

$$\frac{\rho_p \dot{r} c_p x^*}{k_g} = \ln\left[1 + \frac{(T_{eff} - T_s) g_f}{T_s - T_0 - H_s/c_p - \dot{q}_R/\rho_p \dot{r} c_p}\right] \tag{9}$$

Combining Eq. (9) with the flow-chemical-reaction mass balance for thin flame, $\rho_p \dot{r} = K_r p^2 x^*$, leads to the final burn rate equation shown in

$$\rho_p \dot{r} = \sqrt{\frac{k_g}{c_p} K_{r,eff} p^2 \ln\left[1 + \frac{(T_{eff} - T_s) g_f}{T_s - T_0 - H_s/c_p - \dot{q}_R/\rho_p \dot{r} c_p}\right]} \tag{10}$$

The procedure for calculating T_{eff} and $K_{r,\,eff}$ is same as earlier.

3.3. Radiative flux

Following the derivation in Brewster [31] (p218–224) the intensity of radiation from the cloud of Al/Al_2O_3 particles reaching the

propellant surface (I_0) is taken as the product of the total emission factor ($\epsilon' \approx K\Delta s$, for small $K\Delta s$, where K is the extinction coefficient and Δs is the path length) and the total emissive intensity function for a black body ($I_b = \sigma T_p^4$, where T_p^4 is the particle temperature). The coefficient K is the product of extinction cross section ($C = Q\pi d_{Al}^2/4$, where Q is the efficiency factor, taken as unity here) and the number of emitting particles per unit volume ($N_0 = 6\rho_g f_{Al}/\rho_{Al}\pi d_{Al}^3$, where ρ_g is the representative gas density, ρ_{Al} and f_{Al} are the particle density and mass fraction). The net radiative flux (q_R) to the surface is set out in Eq. (11). The radiative loss from the propellant surface emission is neglected as it is much smaller than the gas and condensed phase fluxes. Also, as shown later, the particle radiation becomes significant only for sub-micron Al sizes - a combined effect of particle ignitability and number density (note the inverse relation between radiation and particle size in Eq. 11).

$$\dot{q_R} = \pi\epsilon'\sigma T_p^4 = \pi K\Delta s\sigma T_p^4 = \pi C_s N_0 \Delta s\sigma T_p^4 = \left[\frac{3\pi}{2}\frac{\rho_g f_{Al}}{\rho_{Al} d_{Al}}\right]\Delta s\sigma T_p^4 \tag{11}$$

$$\Delta s = Cx^*(p/20)^{0.5}; \quad C \sim 80$$

The Al particle emission temperature (T_p) is taken as equal to the flame temperature, T_f corresponding to the binder-matrix coated AP particle, since sub-micron particles can be expected to equilibrate with the surrounding gases almost instantaneously. The path length is taken as proportional to the flame thickness (x^*) with an additional pressure dependence - $\Delta s = Cx^* p^m$, where p is taken in atm and C is constant. The term p^m is to account for the variation of extinction coefficient with pressure and a value of $m = 0.5$ captures the experimental results reasonably accurately. This effect can also be interpreted as the variation in the effective number of particles radiating to the propellant surface.

3.4. Agglomeration

Fine particles tend to agglomerate, especially in reacting environments. Since conventional Al particles are known to oxidize far away from the surface and not actively affect the propellant burn rate, agglomeration effects were not considered important as far as propellant ballistics is concerned. But with use of submicron-Al and the fact that the radiation contribution from these particles is strongly dependent on the particle size (see Eq. 11), near surface agglomeration effects must be accounted for in a model for burn rate prediction. For example, both 18 nm [1] and 0.1 μm Al particles [3] increase the burn rate by a factor of 4–5 (compared to the base propellants with CAl). This indicates that, in addition to thermo-chemical and radiation effects, agglomeration of fine-Al start to play a role in determining the burn rate enhancement. Further, Dokhan et al. [6] have reported experimental results for propellants by varying the ratio of conventional to sub-micron Al to show that significant enhancement in burn rate (factor of 2–3) can be achieved by replacement of just 20% of conventional Al with UFAl clearly showing that there is a trade-off due to agglomeration. Similar studies have also been reported in [30] - 3% and 7.5% 0.15 μm Al with 15% total Al (rest is CAl).

3.5. Results

The MATLAB code used for implementation of the *HeQu1-D* model (base code available for download from https://home.iitm.ac.in/varuns/) is extended to include the radiation model and agglomeration effects (details later). Local extinction and related effects on homogenization are accounted for using the same iterative calculation procedure as in HeQu1-D (see [10] for details).

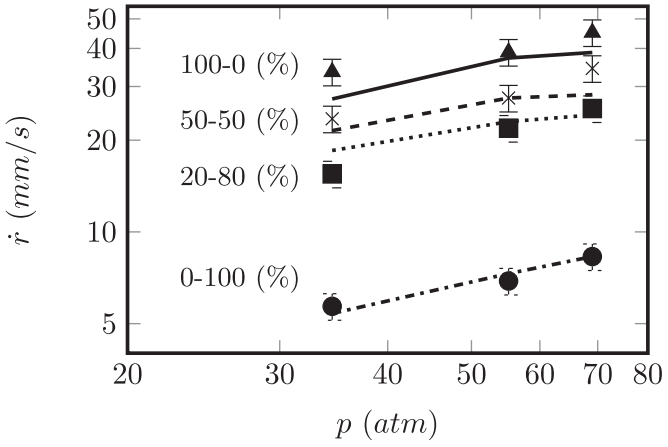

Fig. 9. Comparison of predicted burn rate results for propellants from [6] with 80/20% - 400/82.5 μm AP and 0.1/30 μm Al in different proportions.

By assuming that the role of agglomeration is negligible with 20% UFAl (80% CAl), burn rates were calculated for propellant with 80/20% 400/82.5 μm from [3]. The constant C in the radiation terms was calibrated to obtain reasonable match at 34.5 atm for this propellant and the same value was used throughout. But for 50–50% and 100% UFAl burn rates were over predicted by a large factor (2–3 times). By taking the particle number density corresponding to 20% UFAl substitution as the critical value beyond which agglomeration effects become important, the modified particle diameter is taken to increase by a factor of N/N_0, where N_0 and N are the critical (corresponding to 20% UFAl) and actual Al number densities. With number density values of 1.9 (20% UFAl - N_0), 4.2 (50% UFAl) and 6.9 (100% UFAl) $\times$ 10^{20} fine-Al particles per m^3 the factors are 2.2 (50% UFAl) and 3.6 (100% UFAl) for propellants from [6]. Burn rate results for these three propellants along with experimental results are shown in Fig. 9 and the agreement is found to be reasonable.

Figure 10 (a) and (b) shows the radiative, surface and convective heat fluxes and the corresponding burn rates for 400 and 82.5 μm particles at 69 atm for propellants shown in Fig. 9. With only CAl, the radiative flux is negligible compared to the other two terms for both the particles. As the fraction of UFAl is increased the contribution from radiation increases - this effect is very significant for 400 μm particles as compared to 82.5 μm particles as the flame temperature of the former is significantly higher than the latter (see Fig. 8) and the radiation contribution goes as T_f^4. With 18% UFAl, the radiation received by the 400 μm particle is 120 MW/m^2 and the corresponding burn rate is about 65 mm/s. The surface heat release rate per unit area ($q_s = \rho_p \dot{r} H_s$) for this particle is also very high (50 MW/m^2) as the decomposition is highly exothermic (due to AP). The convective flux is negligible compared to radiation and surface contributions. It is as if the 400 μm particle for the 18% UFAl case is undergoing *radiation dominated ablation*. The same is applicable to the cases with 9% and 3.6% UFAl. All three fluxes are much lower in the case of 82.5 μm as compared to 400 μm particles due to fuel richness and lower flame temperature. Radiation contribution for 82.5 μm particles also increases with increase in UFAl fraction, but not to the same extent as that for 400 μm particles. Convective flux dominates in the case of 82.5 μm particles and the surface heat (q_s) is negative as the fraction of HTPB (21.1%) and Al (34.5%) are large compared to AP (44.4%). Since bi-modal Al results are not available from [1], the critical number density and hence the agglomeration factors cannot be deduced - but a value of 10 for 18 nm particles give accurate predictions. From this, the critical fraction at which agglomeration effects become negligible

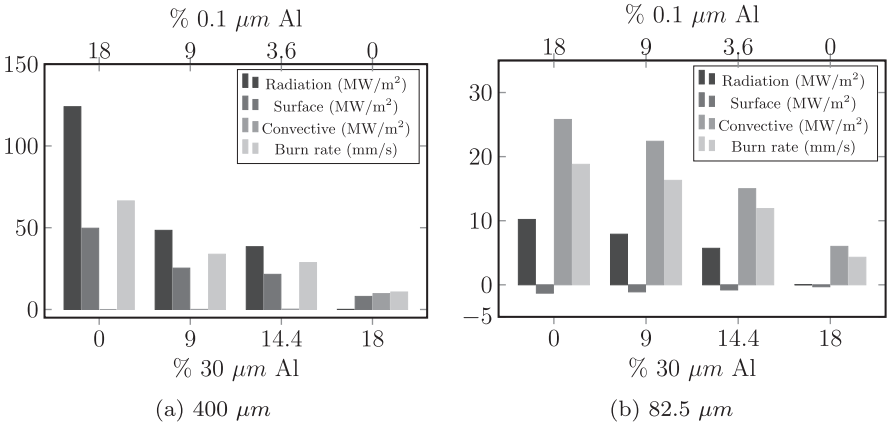

Fig. 10. Radiative, surface and convective fluxes and corresponding burn rates of particles constituting the propellants shown in Fig. 9 calculated at 69 atm.

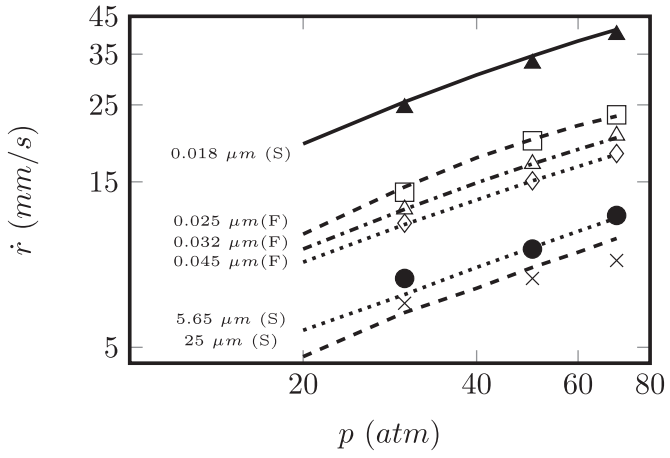

Fig. 11. Comparison of predicted burn rate results for propellants from [1] with 68% 325/54 μm AP in 1:1 ratio and 18% Al of spherical (S) and flaky (F) morphology; marker size represents ± 5%.

is calculated to be 10% for this Al particle size. For propellants with flaky high surface area aluminum, a factor of 17 gives the best results (see Fig. 11). Predictions for propellants with 18 nm and flaky Al from [1] along with experimental results are shown in Fig. 11. Results obtained for bi-modal Al propellants reported in [30] are shown in Fig. 12.

4. Temperature sensitivity

With the introduction of the radiative flux ($\dot{q}_r$) in the surface heat balance (Eq. 8), the closed form expression for temperature sensitivity is as given by

$$\sigma_P = \frac{B}{2(T_s - T_0 - H_s/c_p)(1+B)\ln(1+B) + \frac{RT_s^2}{E_s}(g_f + B) + R_{\sigma_p}} \tag{12}$$

where,

$$R_{\sigma_p} = (B - 2(1+B)ln(1+B))\dot{q}_r/\rho_p \dot{r} c_p$$

This expression for σ_p shares some features with those discussed by Cohen-Nir [21], Cohen and Flanigan [22] - particularly, the terms involving $(T_s - T_0 - H_s/c_p)$ and RT_s^2/E_s in the denominator. The effects of various parameters like AP particle size distribution, presence of Al etc., as predicted by BDP-based models are discussed in detail by Cohen [22]. The conclusions are limited partly by the inability of the models to predict burn rates of wide-distribution propellants (pointed out by Cohen himself) and the effect of impurities in AP (likely to have been the dominant factor).

The term controlling σ_p of aluminized-binder-matrix coated AP particle will be $(T_s - T_0 - H_s/c_p)$ and $\dot{q}_r/\rho_p \dot{r} c_p$. Since $\dot{q}_r$ is negligible compared to other flux terms in propellants with conventional Al, the σ_p behavior is similar to classical non-aluminized propellants. This result is consistent with the observations of Cohen and Flanigan [22]. Predicted temperature sensitivity for TP-H1148 (space shuttle booster) is 0.07 %/K. The reported experimental value is 0.11 %/K. It is important to note that the Kerr-McGee AP used contains 80 ppm potassium, 45 ppm of sodium and several other metals in much less concentration [25] and the σ_p can be expected to higher than that of pure AP. This is most likely the reason for the difference between the value predicted by theory and experiment.

As the fraction of UFAl substituted for CAl increases so do $\dot{q}_r$ and T_s. Depending on whether H_s/c_p is positive (AP rich) or negative (binder rich), σ_p will attain a peak at a certain level of UFAl substitution. Therefore σ_p of propellants with UFAl can be expected to have a non-monotonic behavior with increasing UFAl fraction depending on the relative magnitude of increase in $\dot{q}_r$ and T_s and the sign of H_s/c_p. This result goes beyond the observations in [22], where it is concluded that the σ_p can be expected to increase with a decrease in Al particle size. While this is also observed here, beyond a critical UFAl concentration which depends on the AP distribution, a non-monotonic behavior is predicted. This is due to agglomeration modulated radiation effects which are not accounted for in earlier models.

Predicted results for propellants from [6,30] are shown in Fig. 13. Temperature sensitivity of all propellants with 100% CAl is comparable to conventional high energy AP/HTPB only propellants and has a value of about 0.06 %/K at 69 atm. As the fraction of UFAl substituted for CAl is increased, σ_p increases first and then decreases - consistent with the observation made earlier. Clearly for propellants shown in Fig. 13, at 100% UFAl, the effect of T_s starts counteracting the effect due to $\dot{q}_r$ leading to decrease of σ_p compared to cases with lower UFAl fractions. It is interesting to note that in the presence of significant radiation flux the σ_p of propellant can be higher than that of AP.

Available data on the variation of σ_p with addition of Al is scarce, let alone combined data set with properties of AP used and hence comparison with experimental results is not possible. A misconception is prevalent in the literature that the increase in propellant thermal conductivity with Al addition is responsible for the change in combustion behavior in general and σ_p in particular. Note that the predicted results shown in Fig. 13 are not affected

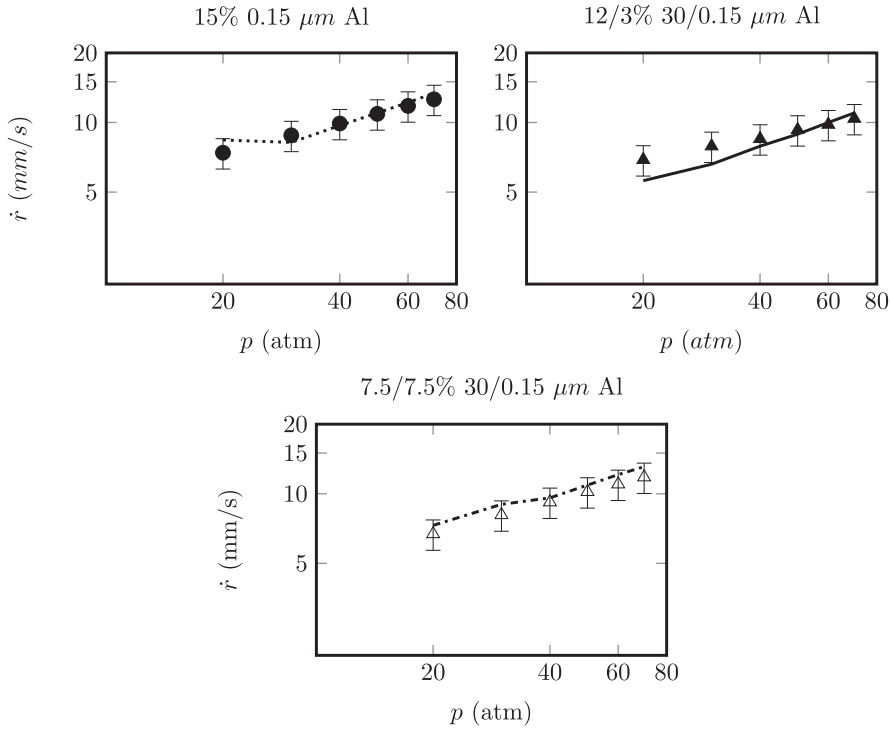

Fig. 12. Comparison of predicted burn rate results for propellants from [6] with 400/82.5μm 50/50 AP (left) and 60/40 AP (right) and different Al sizes.

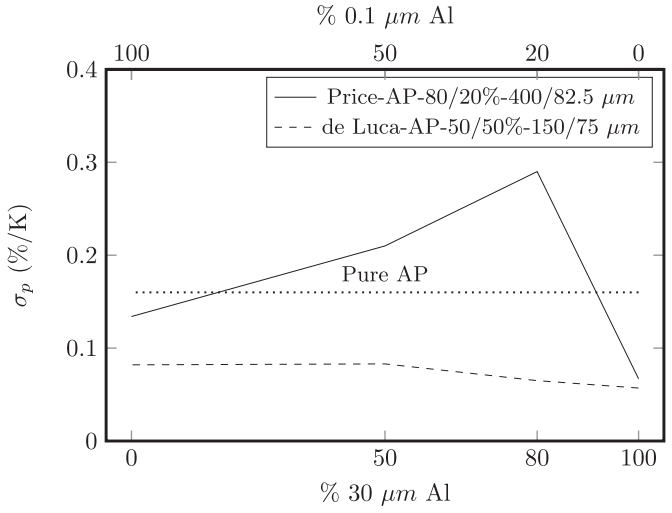

Fig. 13. Effect of UFAl fraction on temperature sensitivity of propellants.

by propellant thermal conductivity - from the surface heat flux balance (Eq. 8) it is clear that the steady burn behavior is not dependent on the thermal conductivity of the propellant. Therefore Al influence on σ_p is through the surface temperature and enthalpy change, in addition to radiation.

5. Free parameter determination via calibration

Accurate predictions without free parameters is the strength of *HeQu1-D* model. A question that comes up is whether such a claim be made for the *extended HeQu1-D model*? Introduction of the radiation and agglomeration models brings with it three additional parameters - two constants (C and m) in the expression for path length and the critical particle number density for agglomeration (N_0). The two constants C and m are calibrated using experimental results of one propellant with sub-micron aluminum and values of 80 and 0.5 are chosen. For other propellants the same values are used and the predictions are found to be reasonable. Hence the values of these constants are not dependent on the choice of a particular propellant for calibration. Use of fine-AP/HTPB/Al premixed propellant burn rate data for calibrating these constants can further improve the confidence levels in predictions. By systematic substitution of increasing fractions of sub-micron sized spherical/flaky Al with and without CAl in premixed propellants the critical agglomeration number density can be estimated from the burn rate data. Similar to the parameter estimation process used for non-aluminized AP/HTPB propellants described in [10], the one dimensional nature of the regression of premixed propellants will provide the necessary robustness and confidence in the values of the estimated constants for aluminized propellants as well. Also using the premixed propellant data the fraction of intermediate nominal size Al (1–10 μm) oxidizing close to the surface can be estimated. Same strategy can be used for incorporating the effects of burn rate catalysts and inhibitors.

6. Conclusions

The *HeQu1-D* framework is extended to account for the effect of aluminum in composite propellant combustion. The assumption that CAl plays a passive role is shown to lead to accurate burn rate predictions. Catalyst effects are also incorporated by modifying the gas phase activation energy and shown to capture the effect of micro and nano-sized Fe_2O_3. This procedure can be used for other burn rate enhancing catalyst like CC, ferrocene etc., as well. Thermo-chemical, radiation and agglomeration effects due to substitution of CAl with sub-micron Al particles are shown to explain the observed burn rate enhancement. Predicted burn rates agree well with the available experimental results for sub-micron Al. With 100% UFAl substitution in place of CAl, the coarse AP particles burn at very high rates (>50 mm/s) akin to radiation dominated ablation with very little influence of convective heat

transfer. Temperature sensitivity variation with CAl and UFAl are presented - the need for further experiments, especially for AP used in propellant making is clearly brought out. Experimental studies along the lines suggested in this work can significantly enhance the predictive capability of the theory.

Acknowledgments

The authors thank Mr. Zaved M S (IIT Madras) and Mr. Vishal Wadhai (IIT Madras) for their contributions to the MATLAB® code development.

References

[1] S. Verma, P. Ramakrishna, Effect of specific surface area of aluminum on composite solid propellant burning, J. Propuls. Power 29 (5) (2013) 1200–1206.
[2] A. Ishihara, M. Brewster, T. Sheridan, H. Krier, The influence of radiative heat feedback on burning rate in aluminized propellants, Combust. Flame 84 (1-2) (1991) 141–153.
[3] A. Dokhan, E. Price, R. Sigman, J. Seitzman, The effects of al particle size on the burning rate and residual oxide in aluminized propellants, 37th AIAA/ASME/SAE/ASEE Joint Propulsion Conference and Exhibit, Joint Propulsion Conferences, American Institute of Aeronautics and Astronautics (2001), p. 3581.
[4] K. Ishitha, P. Ramakrishna, Studies on the role of iron oxide and copper chromite in solid propellant combustion, Combust. Flame 161 (10) (2014) 2717–2728.
[5] E.W. Price, R. Sigman, J. Sambamurthi, C. Park, Behavior of aluminum in solid propellant combustion, Technical Report, Georgia Inst of Tech Atlanta School of aerospace Engineering, 1982.
[6] A. Dokhan, E. Price, J. Seitzman, R. Sigman, The effects of bimodal aluminum with ultrafine aluminum on the burning rates of solid propellants, Proc. Combust. Inst. 29 (2) (2002) 2939–2946.
[7] B. Miles, J. Rackham, The effect of aluminum particle size distribution on tp-h1148 propellant slag, AIAA, ASME, SAE, and ASEE, Joint Propulsion Conference and Exhibit, 32 nd, Lake Buena Vista, FL, American Institute of Aeronautics and Astronautics (1996), p. 3271.
[8] A. Dokhan, E. Price, J. Seitzman, R. Sigman, The ignition of ultra-fine aluminum in ammonium perclorate solid propellant flames, 39th AIAA/ASME/SAE/ASEE Joint Propulsion Conference and Exhibit, American Institute of Aeronautics and Astronautics (2003).
[9] D.S. Sundaram, P. Puri, V. Yang, A general theory of ignition and combustion of nano-and micron-sized aluminum particles, Combust. Flame 169 (2016) 94–109.
[10] S. Varunkumar, M. Zaved, H. Mukunda, A novel approach to composite propellant combustion modeling with a new heterogeneous quasi one-dimensional (HeQu1-D) framework, Combust. Flame 173 (2016) 411–424.
[11] N.S. Cohen, A pocket model for aluminum agglomeration in composite propellants, AIAA J. 21 (5) (1983) 720–725.
[12] S. Gallier, A stochastic pocket model for aluminum agglomeration in solid propellants, Propellants, Explos., Pyrotech. 34 (2) (2009) 97–105.
[13] T. Jackson, F. Najjar, J. Buckmaster, New aluminum agglomeration models and their use in solid-propellant-rocket simularions, J. Propuls. Power 21 (5) (2005) 925–936.
[14] V. Srinivas, S.R. Chakravarthy, Computer model of aluminum agglomeration on burning surface of composite solid propellant, J. Propuls. Power 23 (4) (2007) 728–736.
[15] M. Beckstead, A summary of aluminum combustion, Technical Report, Brigham Young Univ Provo Ut, 2004.
[16] H. Yang, W. Yoon, Modeling of aluminum particle combustion with emphasis on the oxide effects and variable transport properties, J. Mech. Sci. Technol. 24 (4) (2010) 909–921.
[17] K.P. Brooks, M.W. Beckstead, Dynamics of aluminum combustion, J. Propuls. Power 11 (4) (1995) 769–780.
[18] J. Widener, M. Beckstead, Aluminum combustion modeling in solid propellant combustion products, AIAA Paper 3824(1998).
[19] G. Lengelle, J. Duterque, J. Trubert, Physico-chemical mechanisms of solid propellant combustion (Solid propellant chemistry, combustion, and motor interior ballistics A 00-36332 09-28), Progress in Astronautics and Aeronautics, 185, American Institute of Aeronautics and Astronautics, Inc., Reston, VA, 2000, pp. 287–334.
[20] M. Beckstead, A model for solid propellant combustion, Symp. (Int.) Combust. 18 (1) (1981) 175–185.
[21] E. Cohen-Nir, Temperature sensitivity of the burning rate of composite solid propellants, Combust. Sci. Technol. 9 (5-6) (1974) 183–194.
[22] N.S. Cohen, D.A. Flanigan, Mechanisms and models of solid-propellant burn rate temperature sensitivity: a review, AIAA J. 23 (10) (1985) 1538–1547.
[23] F. Blomshield, J. Osborn, Nitramine composite solid propellant modeling, 26th Joint Propulsion Conferences, Orlando, FL, USA, American Institute of Aeronautics and Astronautics (1990), p. 2311.
[24] T.L. Boggs, D.E. Zurn, The temperature sensitivity of the deflagration rates of pure and doped ammonium perchlorate, Combust. Sci. Technol. 4 (1) (1971) 227–232.
[25] K.F. Miks, Solid propellant ingredient reclamation and reuse, JANNAF Safety and Environmental Protection Subcommittee Meeting, Las Cruces, New Mexico (2003) (1993).
[26] R.R. Miller, Effects of particle size on reduced smoke propellant ballistics, AIAA paper 1096(1982).
[27] G. Marothiya, C. Vijay, K. Ishitha, P. Ramakrishna, An effective method to embed catalyst on AP and its effect on the burn rates of aluminized composite solid propellants, Combust. Flame 182 (2017) 114–121.
[28] M.L. Gross, M.W. Beckstead, Diffusion flame calculations for composite propellants predicting particle-size effects, Combust. Flame 157 (5) (2010) 864–873.
[29] S. Verma, P. Ramakrishna, Activated charcoal – a novel burn rate enhancer of aluminized composite propellants, Combust. Flame 157 (6) (2010) 1202–1210.
[30] L. De Luca, L. Galfetti, F. Severini, L. Meda, G. Marra, A. Vorozhtsov, V. Sedoi, V. Babuk, Burning of nano-aluminized composite rocket propellants, Combust., Explos. Shock Waves 41 (6) (2005) 680–692.
[31] M.Q. Brewster, Thermal radiative transfer and properties, John Wiley & Sons, 1992.
[32] B. Smith, Block II SRM conceptual design studies final report. Volume I, Book 1, conceptual design package [microform], Morton Thiokol, Inc., Wasatch Operations, Space Division Brigham City, Utah, 1986.